Time-reversibility, instability and thermodynamics in n-body systems interacting with long-range potentials

Time-Reversibility, Instability and Thermodynamics in *N*-body Systems Interacting with Long-Range Potentials

Nobuyoshi Komatsu

Department of Mechanical Systems Engineering, Kanazawa University, Kakuma-machi, Kanazawa, Ishikawa 920-1192, Japan

Abstract

Long-range attractive potentials cause self-gravitating *N*-body systems to exhibit not only chaotic behavior but also peculiar features such as gravothermal catastrophe, negative specific heat and nonextensive statistical mechanics. Especially when its potential energy is significantly dominated, a system should gradually evolve from quasi-equilibrium states through collapses to core-halo states. In dynamical evolution, velocity distributions are generally expected to monotonically relax from non-Gaussian towards Gaussian (Maxwell–Boltzmann) distributions. To clarify the velocity relaxation, we numerically examine the long-term evolution of a self-gravitating *N*-body system enclosed in a spherical container with adiabatic walls. We found that the velocity distribution non-monotonically relaxes from a non-Gaussian distribution to a Gaussian-like distribution when a core forms rapidly through the collapse process.

1. Introduction

Chaos is considered to be one of the origins of irreversibility appearing in macroscopic systems, such as *N*-body systems [1]. Accordingly, stability of systems has been extensively examined numerically, especially in *N*-body systems interacting with short-range potentials. However, it is known that numerical irreversibility due to round-off errors may behave as if it were physical irreversibility, although it is not in fact physical. Numerical irreversibility in standard *N*-body simulations [2] makes it difficult to investigate physical irreversibility numerically. Recently, to clarify numerical irreversibility in classical molecular-dynamics (MD) simulations with short-range potentials, the present author *et al.* proposed a new method based on a bit-reversible algorithm [3] and controlled noise [4-6]. The bit-reversible algorithm, which combines the Verlet algorithm with space discretization using integer arithmetic, is free from round-off errors and is completely time-reversible and therefore can detect any irreversibility in MD simulations. By means of the new method, the Boltzmann *H*-function and instability of the system have been

investigated, through the Loschmidt reversibility paradox based on a velocity inversion technique [4,5]. It was clearly demonstrated that numerical irreversibility due to round-off errors correlated with the process of relaxation and the magnitude of noise, and that the irreversibility propagated through collisions between particles. For example, an expansion shock wave appearing in the bit-reversible MD simulation disappears dramatically and turns into an isentropic expansion wave when controlled noise is intentionally added to the system [6].

The influence of round-off errors should be a more serious problem in N-body systems interacting with long-range potentials, e.g., self-gravitating systems [7]. For instance, in a typical star-rich cluster with a million stars, each star feels enough of the granularity of the gravitational field of the other stars that the consequent perturbations lead to a total loss of memory of the initial conditions of its orbit [8]. In self-gravitating N-body simulations, numerical fluctuations due to round-off errors could behave as if they were the physical perturbations, as for systems with short-range potentials. Therefore, the present author *et al*. have investigated numerical irreversibility and instability of a self-gravitating system [9,10]. Under the restriction of constant initial potential energy, the numerical irreversibility is found to increase rapidly with decreasing initial kinetic energy or total energy. In other words, the lower the initial kinetic energy or total energy, the earlier the memory of the initial conditions is lost. Moreover, the memory loss time, i.e., when the simulated trajectory completely forgets its initial conditions, increases approximately linearly with the Lyapunov time. It is shown that propagation of numerical irreversibility or loss of reversibility depends on both the energy state of the system and the instability affected by the softening parameter [9,10].

Due to long-range attractive potentials, chaotic self-gravitating N-body systems exhibit several peculiar features, e.g., gravothermal catastrophe, negative specific heat and nonextensive statistical mechanics [11,12]. In particular, negative specific heat causes thermodynamic instability during dynamical evolution of the system and has been investigated theoretically and numerically from a thermodynamic viewpoint [13-16]. The present author *et al*. have examined a self-gravitating N-body system enclosed in a spherical container with adiabatic and non-adiabatic walls [15]. (For a nonequilibrium process, a particle reflected at the non-adiabatic wall is cooled to mimic energy loss by reflecting walls.) It is clearly demonstrated that a negative specific heat occurs not only in microcanonical ensembles but also in the nonequilibrium process with energy loss. The dependence of the temperature on energy, i.e., the ε–T curve, varies from the ε–T curve for a microcanonical ensemble, tending towards a common curve with increasing cooling rate. Surprisingly, the common curve agrees with the ε–T curve for stellar polytropes assuming hydrostatic equilibrium states, especially for a polytrope index of $n \sim 5$ [15]. This result is consistent with gravothermal instability since, for $n > 5$, a stellar polytrope within an adiabatic wall exhibits gravothermal instability [13]. (Using semipermeable reflecting walls, the above model has been applied to further strong nonequilibrium processes with mass and energy loss, i.e., the so-called evaporation process [16].)

However, velocity distributions and velocity relaxations have not yet been extensively discussed for long-term nonequilibrium processes, except for a few studies [17,18], although they should play an important role in the thermodynamic properties and irreversibility of the system [19,20]. For example, Iguchi *et al*. [17] proposed universal non-Gaussian velocity distributions for a spherical collapse in a violent gravitational process of a collisionless stage ($t < \tau_r$), while Ispolatov *et al*. [18] discussed Gaussian velocity distributions in core-halo states in a collisional stage ($t >> \tau_r$). (Here τ_r represents the relaxation time, which is driven by the two-body encounter [11]. A Gaussian distribution means a Maxwell–Boltzmann distribution.) These works suggest that long-range attractive interacting systems should finally relax towards a Boltzmann-like state thorough a collapse process [20]. In general, we expect that velocity distributions monotonically relax from a non-Gaussian distribution towards a Gaussian distribution (Fig.1). However, interesting observation data of open stellar clusters has been reported recently by

Carvalho *et al.* [21]. They reported that the radial velocity distribution of old open stellar clusters changes from a non-Gaussian distribution to a higher non-Gaussian distribution (not to a Gaussian distribution), with increasing age of the clusters. In other words, the velocity distribution further deviates from Gaussian for older clusters.

In the present study, to clarify the properties of self-gravitating *N*-body systems, we numerically examine the long-term dynamical evolution of a system, from an early relaxation to a collapse, focusing on velocity relaxations [20]. For this purpose, we examine a cold collapse process of a self-gravitating system under the restriction of constant mass and energy. To simulate the cold collapse process, we employ a typical small *N*-body system which has been analyzed in detail by Ispolatov and Karttunen [18], since the well-studied system is an important benchmark system for examining a collapse theoretically and numerically [20].

The present paper is organized as follows. In Sec. 2, we present the simulation method. In Sec. 2.1, we give a brief review of the numerical techniques for simulating a self-gravitating system enclosed in a spherical container with adiabatic walls. In Sec. 2.2, we briefly review the parameters for the simulations, e.g., the Tsallis entropic parameter, the ratio of velocity moments and the virial ratio. In Sec. 3, we present the simulation results and discuss the velocity relaxation. Finally, we present our conclusions in Sec. 4. In the present paper, typical results of the cold collapse process studied in Refs. [19,20] are reconsidered from the viewpoint of velocity relaxations of a chaotic system with long-range attractive potentials. Note that new *N*-body simulations are carried out, since the ratio of the velocity moments examined in this study is slightly different from that in Refs. [19,20] (see Sec. 2.2 for details).
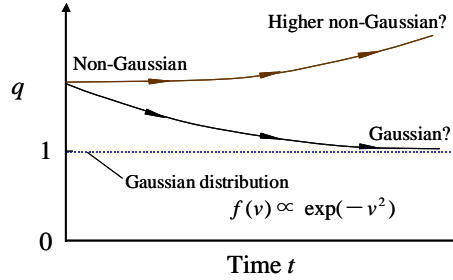

Fig. 1. Schematic diagram of typical velocity relaxations. The vertical axis represents a deviation q of the velocity distribution from the Gaussian distribution. In this figure, $q=1$ corresponds to the Gaussian velocity distribution $\sim \exp(-v^2)$, and $f(v)$ represents the velocity distribution function. The velocity distribution is generally expected to relax from a non-Gaussian distribution to a Gaussian distribution monotonically. However, an interesting observation result has been reported recently that exhibits a tendency to a higher non-Gaussian distribution [21].

2. Simulation methods

In this section we briefly review the simulation methods, according to Ref. [20].

2.1. N-body simulations

To simulate self-gravitating *N*-body systems, we consider a typical situation known as the Antonov problem (Fig. 2): i.e., we consider a self-gravitating system consisting of *N* point-particles enclosed in a spherical container of radius *R* with adiabatic walls [9,10,19,20]. By means of the Verlet algorithm (i.e.,

leapfrog algorithm), we integrate a set of classical equations of motion for the particles interacting through the Plummer softened potential Φ [11] :

$$\Phi = -1/(r+r_0)^{1/2} \qquad (1)$$

where r and r_0 represent the distance between particles and the softening parameter, respectively. r_0 is employed to avoid numerical singularity. In our simulations, the softening parameter is set to be $r_0 = 0.005R$. Note that r_0 affects the instability of the system [10]. For example, when r_0 is large, the scattering is small. In contrast, when r_0 is small, as for pure gravitational potentials, the scattering is large. Accordingly, when r_0 is small, the Lyapunov time should be short since the system is more unstable. We checked the instability of the system for this study, i.e., the Lyapunov time, and set $r_0 = 0.005R$, since the Lyapunov time of the system with $r_0 = 0.005R$ is sufficiently shorter than the relaxation time.

The total energy E of the system is defined as $E = E_{KE} + E_{PE}$ where E_{KE} and E_{PE} represent kinetic energy and potential energy, respectively. The total rescaled energy ε is defined as

$$\varepsilon = ER/(GM^2) = ER/(Gm^2N^2) \qquad (2)$$

where G, M and m represent the gravitational constant, the total mass and the mass of each particle, respectively. In this study, the units of time t and velocity v are $[R^3/(Gm)]^{1/2}$ and $(Gm/R)^{1/2}$, respectively [10,20]. The units are set to be $G = R = m = 1$, to ensure generality of the system. We assume that the kinetic energy corresponds to the temperature T of the system and that the Boltzmann constant $k_B=1$. As a result, in our units, the temperature is given by $T = 2\varepsilon_{KE}/(3k_B) = 2\varepsilon_{KE}/3$, where ε_{KE} is the rescaled kinetic energy. In the present simulation, the total energy ε is set to be -1.0, to simulate a typical gravity-dominated system. A total energy of $\varepsilon = -1.0$ is sufficiently lower than the collapse energy $\varepsilon_{coll} = -0.339$ for the present system with an adiabatic wall [18]. (In Ref. [20], we also discuss the simulation result with various ε ranging from -0.6 to -1.2.)
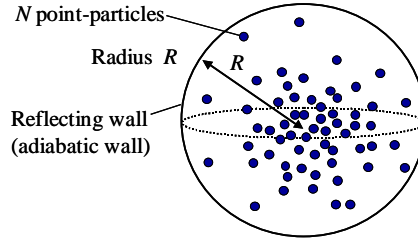

Fig. 2. Setup for the Antonov problem. As a typical simple model, we consider a self-gravitating system consisting of N point-particles enclosed in a spherical container of radius R with adiabatic walls. The total energy E and the number N of particles are fixed during simulations.

To consider a typical small N-body system, the number N of particles is set to be 125. Accordingly, in our units, the crossing time τ_c and the relaxation time τ_r are evaluated as $\tau_c \sim 0.2$ and $\tau_r \sim 0.5$ [20]. However, it takes a much longer time for the collapse to be completed in a core-halo state. For example, the complete collapse time in a system with $N = 100–200$ particles is approximately $10^3–10^4\tau_c$ [22] and, therefore, the collapse time of the present study is the order of $10^2–10^3$ in our units. Note that τ_c corresponds to the free-fall time. τ_c and τ_r can be evaluated as $\tau_c \sim 1/(G\rho)^{1/2}$ and $\tau_r \sim (0.1N/\ln N)\,\tau_c$, respectively, where ρ represents the density assuming a uniform density profile [11,13].

The initial density profile is based on the Plummer model, $\rho \sim (1+r^2/a^2)^{-5/2}$ [11], since this model is suitable for simulating stellar clusters. The initial velocity is set to be small to simulate cold and

nonequilibrium initial-states for cold collapse processes: i.e., the initial kinetic energy is set to be negligible, smaller than the order of 1% of the total energy. (Initially, all the particles have a small equal speed but with a random direction.) In the above setup, microcanonical ensemble simulations are carried out using 30 simulations with different initial configurations [20].

2.2. Parameters for simulations

In general, the Boltzmann H-function has been widely employed to examine velocity relaxation. However, the temperature (i.e., kinetic energy) of self-gravitating systems increases during their dynamical evolution because of gravitational potentials. Therefore, we did not employ the Boltzmann H-function, since it depends on temperature. Instead, we employed the following two parameters to examine whether the simulated velocity distribution function is Gaussian.

The first parameter is the Tsallis entropic parameter q based on a q-Gaussian distribution function [12]. The one-component q-Gaussian distribution function is defined as

$$f_q(v) = A \exp_q (-Bv^2) = A [1-B(1-q)v^2]^{1/(1-q)} \qquad (3)$$

$$\exp_1 (-Bv^2) = \exp (-Bv^2) \qquad (4)$$

where q is the Tsallis entropic parameter at time t [12]. When $q = 1$, this function is reduced to the Gaussian form exactly. A is a normalization parameter and B corresponds approximately to the inverse of temperature. In the present study, these temporal parameters are determined by fitting with a simulated velocity distribution function $f_{sim}(v)$ [20]. Note that $f_{sim}(v)$ is first averaged over 30 simulations. After the ensemble average is obtained, $f_{sim}(v)$ for $t < 30$ and $t > 30$ are time-averaged over $\Delta t = 0.1$ and $\Delta t = 2$, respectively, to determine the distribution function more clearly.

The second parameter is the normalized ratio of velocity moments $VM(t)$. The ratio of velocity moments $vm(t)$ is first defined as

$$vm(t) = < v_i^2 >^2 / < v_i^4 > \qquad (5)$$

where v_i and $< X >$ represent the velocity of the i-th particle and the mean of X at time t, respectively. The ratio of velocity moments varies from an initial value towards a specific value $vm_G (= 1/3)$ corresponding to the Gaussian distribution. Accordingly, we define the normalized ratio of velocity moments as

$$VM(t) = vm(t) / vm_G \qquad (6)$$

When $VM = 1$, the velocity distribution is Gaussian, as for q. It should be noted that in Eq. (5) we employ the one-component velocity v_i of the particles, unlike in Ref. [20]. Therefore, the specific value vm_G for the Gaussian velocity distribution is 1/3. If the speed of the particles is employed, the specific value for the Gaussian (Maxwell–Boltzmann) speed distribution is 0.6, as examined in Ref. [20]. We have confirmed that the fluctuations of $VM(t)$ considered here are slightly larger than $VM_{speed}(t)$, which is computed from the speed of the particles. However, a time-averaged VM approximately agrees with a time-averaged VM_{speed}, when $VM(t)$ and $VM_{speed}(t)$ are time-averaged over $\Delta t = 0.1$. In this paper, the velocity v_i of the particles is employed to define $VM(t)$, since q is determined by fitting with the simulated velocity distribution function.

To observe an equilibrium state, the virial ratio α is defined as

$$\alpha = (2E_{KE} - 4\pi R^3 P_{wall}) / | E_{PE} | \qquad (7)$$

where P_{wall} represents the pressure on the container wall by reflecting particles [10,15,16,18,20]. The virial ratio is 1 if the system is in the virial equilibrium state with pure gravitational potentials. Note that the virial ratio in core-halo states with soft gravitational potentials is not 1 [20], since particles in the core

are well within the softening radius (i.e., the softening parameter r_0), unlike for pure gravitational potentials [18]. For example, the virial ratio defined by Eq. (7) is evaluated as 0.555 in the core-halo state with $\varepsilon = \varepsilon_{\text{coll}} = -0.339$ and $r_0 = 0.005$ [18].

Moreover, we examine the number N_c of core particles of a prescribed radius r_c, instead of temporal density profiles [20]. This is because during a collapse process of small N-body systems, it is difficult to observe the density profile due to strong fluctuations in the position of the high-density parts [18]. In this paper, according to Ref. [18], we count the number N_i of particles within r_c from the i-th particle and find the particle which has the largest N_i. The prescribed radius r_c is set to be 0.01 [20].

3. Results

In this paper, as a typical result, we examine a cold-collapse process with constant mass and energy for $\varepsilon = -1.0$. The details are described in Ref. [20]. (In Ref. [20], we have discussed not only the cold-collapse simulation with various total energies but also evaporation–collapse simulations.)

To examine an overview of dynamical evolution, we first observe time evolutions of T, α and N_c. As shown in Fig. 3, initially ($t < 0.2$), N_c is approximately constant and, therefore, a collapse has not yet started. However, we can confirm that T and α fluctuate significantly. This is because the initial temperature calculated from the initial kinetic energy is extremely low due to our initial setup of the cold collapse simulation. The above time, i.e., $t \sim 0.2$, likely corresponds to the crossing time $\tau_c \sim 0.2$ of the present small system. However, T and α gradually approach specific values. In particular, α gradually approaches 1 for $0.5 < t < 1$. Accordingly, the system is in an approximate virial equilibrium state or a quasi-equilibrium state during this stage. The approaching time, i.e., $t \sim 0.5$, likely corresponds to the relaxation time $\tau_r \sim 0.5$. However, after this stage ($t > 1$), N_c rapidly increases and α gradually deviates from 1. Therefore, we expect that a collapse should start from $t \sim 1$ in the present cold collapse simulation. It should be noted that the deviation of α from 1 is caused by the Plummer softened potential, since the core particles are well within the softening radius r_0 [18]. For $t > 7$, the growth of N_c gradually tends to be slower than that of the early stage. After a delay of several time units, i.e., for $t > 10$, T starts to increase rapidly. This delay has been noted in Ref. [18]. Since the temperature increases in this process, our system discussed here has not yet approached a complete core-halo state [20].

To examine velocity relaxations, we observe VM and q. As mentioned previously, VM and q are 1 when the velocity distribution is Gaussian. Note that VM discussed here is calculated from the velocity of the particles, while VM_{speed} examined in Refs. [19,20] is calculated from the speed of the particles. Although the fluctuations of VM are slightly larger than VM_{speed}, the time-averaged values approximately agree with each other when they are time-averaged over $\Delta t = 0.1$. Therefore, our simulation result in the present paper is consistent with the result in Refs. [19,20], although VM is different from VM_{speed} in Refs. [19,20].

As shown in Fig. 4 (bottom), for $t < 1$, VM and q deviate from 1 (i.e., VM < 1, $q > 1$). This indicates that the velocity distribution is non-Gaussian in the early relaxation process or in the quasi-equilibrium state. In the early relaxation process, the velocity distribution is well fitted with the q-Gaussian distribution for $q > 1$ (e.g., see the top-left panel for $f(v)$ at time $t = 0.5$ in Fig. 4). Thereafter, for $t > 1$, VM and q further deviate from 1. In fact, N_c starts to increase at $t \sim 1$. This suggests that the velocity distribution exhibits higher non-Gaussian distributions, especially when the core forms rapidly in the early collapse process. However, the velocity distribution gradually relaxes toward a Gaussian-like distribution (VM ~ 1, $q \sim 1$) after the core forms sufficiently ($t > 200$) (e.g., see the top-right panel for $f(v)$ at $t = 300$ in Fig. 4).

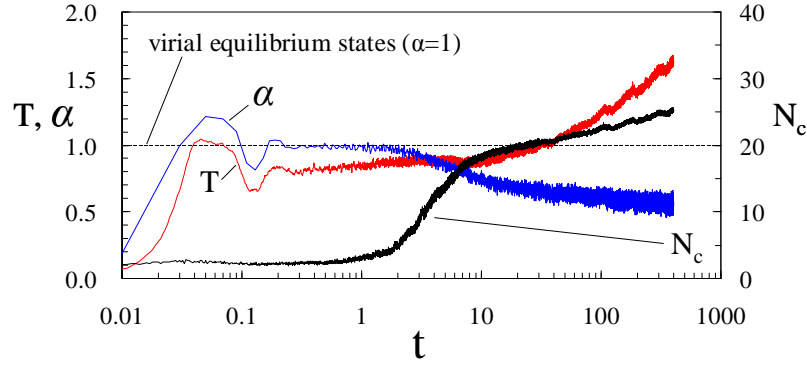Fig. 3. Time evolutions of temperature T, virial ratio α and number N_c of core particles, for $\varepsilon = -1.0$ [20]. $\alpha = 1$ when the system is in the virial equilibrium state. In our units, the crossing time τ_c and the relaxation time τ_r are approximately evaluated as $\tau_c \sim 0.2$ and $\tau_r \sim 0.5$. The complete collapse time is expected to be the order of 10^2–10^3.
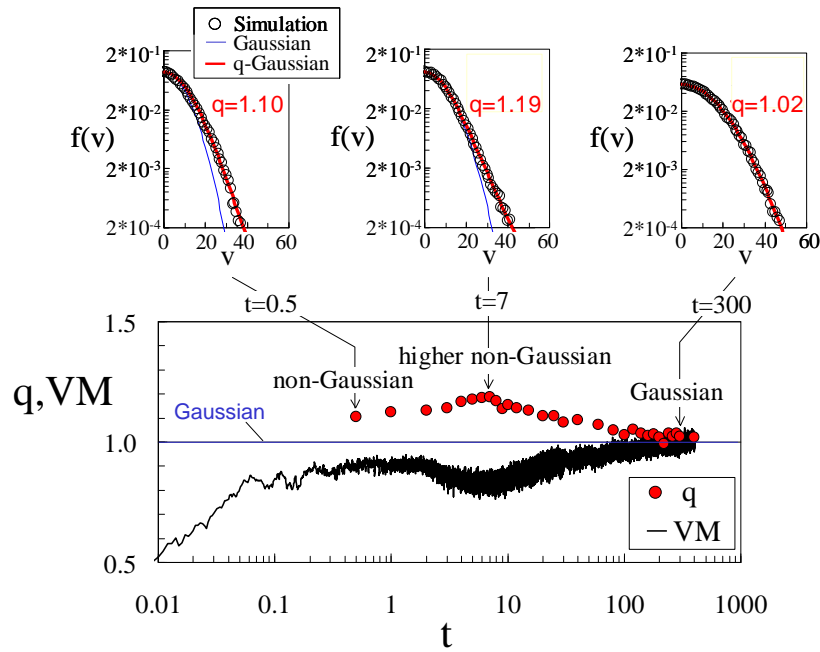

Fig. 4. Time evolutions of the normalized ratio of velocity moments VM and Tsallis entropic parameter q, for $\varepsilon = -1.0$ [20]. When the velocity distribution is Gaussian, VM and q are 1. Typical temporal velocity distribution functions $f(v)$ are shown in the three top-panels (left: $t = 0.5$, middle: $t = 7$, right: $t = 300$). In the three top panels, the open circles represent the simulated velocity distribution functions, while the blue-thin and red-heavy lines represent Gaussian and q-Gaussian functions, respectively. The velocity distribution function is time-averaged, after the ensemble averaged is obtained (see Sec. 2.2). Note that VM shown in the bottom figure is calculated from the velocity of the particles, while VM_{speed} examined in Refs. [19,20] is calculated from the speed of the particles.

Surprisingly, we found that the velocity distribution relaxes from a non-Gaussian distribution towards a Gaussian-like distribution non-monotonically, because of an early collapse process. We clearly show such a transition of the velocity distribution, based not only on q but also on VM. We expect that our simulation result is likely related to the observation data of open stellar clusters [21]. (In Ref. [21], Carvalho *et al.* reported that a radial velocity distribution of the old open stellar clusters varies from a non-Gaussian distribution to a higher non-Gaussian distribution with increasing age of the clusters.)

As discussed above, we focus on the velocity relaxation and examine velocity moments and q, which is calculated from $f(v)$. In fact, we have examined phase-space distribution functions $f(x,v)$. Consequently, $f(x,v)$ of the present system significantly depends on its normalization of both configuration space and velocity space. Accordingly, phase-space distribution functions are not discussed in the present study. Note that energy distributions have been discussed in Ref [20].

In the present cold collapse simulation, the initial velocity distribution is a delta-function-like distribution with negligible small values, to observe variations in velocity distributions clearly. Therefore, the initial setup may affect the deviation of the velocity distribution from Gaussian. To clarify this, we have confirmed that the velocity distribution deviates from Gaussian, even if the initial velocity distribution is a Gaussian-like distribution. Of course, further research is required to clarify whether a collapse plays an important role in the deviation from Gaussian [20].

4. Conclusions

To clarify the strange velocity-relaxation of chaotic N-body systems interacting with long-range attractive potentials (i.e., self-gravitating N-body systems), we have numerically examined long-term evolutions of these systems, from an early relaxation to a collapse [20]. In the present paper, we have focused on a cold-collapse process under a restriction of constant mass and energy. Consequently, the velocity distribution is non-Gaussian in a quasi-equilibrium state or an early relaxation process, when the total energy is lower than the collapse energy. In dynamical evolutions of the system, the velocity distribution further deviates from the Gaussian distribution, especially in an early collapse process, i.e., when the core forms rapidly. However, after the core forms sufficiently, the velocity distribution gradually approaches an approximate Gaussian distribution. It is clearly shown that the velocity distribution evolves from a non-Gaussian distribution ($q = q_1 > 1$) through a higher non-Gaussian distribution ($q > q_1$) to an approximate Gaussian distribution ($q \sim 1$). In other words, the velocity distribution relaxes from a non-Gaussian distribution towards a Gaussian-like distribution non-monotonically. Similar transitions of the velocity distribution have been observed in evaporation–collapse processes [20]. We also found q and VM are suitable for observing the evolution of velocity distributions in a chaotic system with long-range attractive potentials. We have not yet clarified irreversibility. However, our studies present a new approach for examining irreversibility, instability and thermodynamics of N-body systems interacting with long-range attractive potentials.

References

[1] Hoover WG. *Time reversibility, Computer simulation, and Chaos*. 1st ed. World Scientific Publishing Co.; 1999.

[2] Orban J, Bellemans A. Velocity-inversion and irreversibility in a dilute gas of hard disks. *Phys. Lett.* 1967;**24A**:620-1.

[3] Levesque D, Verlet L. Molecular dynamics and time-reversibility. *J. Stat. Phys.* 1993;**72**:519-537.

[4] Komatsu N, Abe T. Numerical irreversibility in time-reversible molecular dynamics simulation. *Physica D* 2004;**195**:391-7.

[5] Komatsu N, Abe T. Noise-driven numerical irreversibility in molecular dynamics technique. *Comput. Phys. Commun.* 2005;**171**:187-196.

[6] Komatsu N, Abe T. Expansion shock waves in the implosion process from a time-reversible molecular-dynamics simulation of a dual explosion process. *Phys. Fluids* 2007;**19**:056103.

[7] Miller MH. Irreversibility in small stellar dynamical systems. *Astrophys. J.* 1964;**140**:250-6.

[8] Heggie DC, Hut P. *The gravitational million-body problem*. 1st ed. Cambridge University press; 2003.

[9] Komatsu N, Kiwata T, Kimura S. Numerical irreversibility in self-gravitating small *N*-body systems. *Physica A* 2008;**387**:2267-2278.

[10] Komatsu N, Kiwata T, Kimura S. Numerical irreversibility in self-gravitating small *N*-body systems. (II). Influence of instability affected by softening parameters. *Physica A* 2009;**388**:639-650.

[11] Binney J, Tremaine S. *Galactic Dynamics*. 1st ed. Princeton University Press; 1987.

[12] Tsallis C. *Introduction to Nonextensive Statistical Mechanics*: *Approaching a Complex World*. 1st ed. Springer; 2009.

[13] Taruya A, Sakagami M. Long-term evolution of stellar self-gravitating systems away from thermal equilibrium: connection with nonextensive statistics. *Phys. Rev. Lett*. 2003;**90**:181101.

[14] Posch HA, Thirring W. Stellar stability by thermodynamics instability. *Phys. Rev. Lett.* 2005;**95**:251101.

[15] Komatsu N, Kimura S, Kiwata T. Negative specific heat in self-gravitating *N*-body systems enclosed in a spherical container with reflecting walls. *Phys. Rev. E* 2009;**80**:041107.

[16] Komatsu N, Kiwata T, Kimura S. Thermodynamic properties of an evaporation process in self-gravitating *N*-body systems. *Phys. Rev. E* 2010;**82**:021118.

[17] Iguchi O, Sota Y, Tatekawa T, Nakamichi A, Morikawa M. Universal non-Gaussian velocity distribution in violent gravitational processes. *Phys. Rev. E* 2005;**71**:016102.

[18] Ispolatov I, Karttunen M. Collapses and explosions in self-gravitating systems. *Phys. Rev. E* 2003;**68**:036117.

[19] Komatsu N, Kiwata T, Kimura S. Relaxation of non-Gaussian velocity distributions in collapses of long-range attractive interacting systems. Abstracts of the 2nd international symposium on Multi-scale Simulations of Biological and Soft Materials (MSBSM2011), p. 22, Kyoto, Japan, 2011.

[20] Komatsu N, Kiwata T, Kimura S. Transition of velocity distributions in collapsing self-gravitating *N*-body systems. *Phys. Rev. E* 2012;**85**:021132.

[21] Carvalho JC, Soaresa BB, Martinsa BLC, Nascimento Jr. JD, Recio-Blancob A, Medeirosa JR. Radial velocities of open stellar clusters: A new solid constraint favouring Tsallis maximum entropy theory. *Physica A* 2007;**384**:507-515.

[22] Ispolatov I, Karttunen M. Anomalously slow phase transitions in self-gravitating systems. *Phys. Rev. E* 2004;**70**:026102.